



1 **Spatial and seasonal variations of leaf area index (LAI) in subtropical secondary**
2 **forests related to floristic composition and stand characters**

3
4 **Wenjuan Zhu^{1,2}, Wenhua Xiang^{1,2,3*}, Qiong Pan^{4,1}, Yelin Zeng¹, Shuai Ouyang^{1,2,3}, Pifeng Lei^{1,2,3},**
5 **Xiangwen Deng^{1,2,3}, Xi Fang^{1,2,3}, Changhui Peng^{5,1}**

6
7 1 Faculty of Life Science and Technology, Central South University of Forestry and Technology,
8 Changsha 410004, Hunan Province, China

9 2 Huitong National Field Station for Scientific Observation and Research of Chinese Fir Plantation
10 Ecosystem in Hunan Province, Huitong 438107, China

11 3 National Engineering Laboratory of Applied Technology for Forestry & Ecology in Southern China,
12 Changsha 410004, China

13 4 Changsha Environmental Protection College, Changsha 410004, China

14 5 Institute of Environment Sciences, Department of Biological Sciences, University of Quebec at
15 Montreal, Montreal, QCH3C 3P8, Canada

16
17 * *Correspondence to:* Wenhua Xiang, Email: xiangwh2005@163.com, Tel.: +86 0731 85623483

18

19



20 **Abstract.** Leaf area index (LAI) is an important parameter related to carbon, water and energy
21 exchange between canopy and atmosphere, and is widely applied in the process models to simulate
22 production and hydrological cycle in forest ecosystems. However, fine-scale spatial heterogeneity of
23 LAI and its controlling factors have not been fully understood in Chinese subtropical forests. We used
24 hemispherical photography to measure LAI values in three subtropical forests (i.e. *Pinus massoniana* -
25 *Lithocarpus glaber* coniferous and evergreen broadleaved mixed forests, *Choerospondias axillaris*
26 deciduous broadleaved forests, and *L. glaber* - *Cyclobalanopsis glauca* evergreen broadleaved forests)
27 during period from April, 2014 to January, 2015. Spatial heterogeneity of LAI and its controlling factors
28 were analysed by using geostatistics method the generalised additive models (GAMs), respectively. Our
29 results showed that LAI values differed greatly in the three forests and their seasonal variations were
30 consistent with plant phenology. LAI values exhibited strong spatial autocorrelation for three forests
31 measured in January and for the *L. glaber* - *C. glauca* forest in April, July and October. Obvious patch
32 distribution pattern of LAI values occurred in three forests during the non-growing period and this
33 pattern gradually dwindled in the growing season. Stand basal area, crown coverage, crown width,
34 proportion of deciduous species on basal area basis and forest types affected the spatial variations in
35 LAI values in January, while species richness, crown coverage, stem number and forest types affected
36 the spatial variations in LAI values in July. Floristic composition, spatial heterogeneity and seasonal
37 variations should be considered for sampling strategy in indirect LAI measurement and application of
38 LAI to simulate functional processes in subtropical forests.



39 **Keywords:** Leaf area index; Spatial heterogeneity; Deciduous species; Generalised additive models
40 (GAMs)

41

42 **1 Introduction**

43 Many fundamental ecological processes in forest ecosystems, such as carbon (C) flux as well as
44 water and energy exchanges, take place between canopy layer and the atmosphere (Brut et al., 2009;
45 GCOS, 2006; Alonzo et al., 2015; Liu et al., 2015b). At finer scale, leaves within canopy are the
46 primary organ to perform a series of physiological activities (i.e. photosynthesis, respiration and
47 evapotranspiration) (Aragão et al., 2005) and physical reactions (i.e. rainfall and radiation interception)
48 (Smith, 1981; Crockford & Richardson, 2000; Aston, 1979). Therefore, the amount of leaves in a forest
49 is the determinant of aboveground ecological processes and ecosystem functions. Leaf area index (LAI),
50 defined as total one-sided leaf area per unit ground surface area (Biudes et al., 2014), is widely used
51 parameter (Kross et al., 2015) to quantitatively describe the vegetation canopy structure (Woodgate et
52 al., 2015), to simulate ecological process models (Sprintsin et al., 2007; Facchi et al., 2010; Brooks et
53 al., 2006; Gonsamo & Chen, 2014) and to reveal tree growth and productivity in forests at stand scale
54 and landscape level (Liu et al., 2015b; Lee et al., 2004). In addition, LAI is listed as one of the essential
55 variables for observation of global climate (Mason et al., 2003; Manninen et al., 2009) and for remote
56 sensing data validation (Asner et al., 2003; Clark et al., 2008). Thus, accurate estimations of LAI value
57 are important to understand ecological processes in forest ecosystems.



58 At present, various direct and indirect methods have been developed to measure LAI in forests.
59 Direct estimation methods including leaf harvest (Clark et al., 2008), allometric equations and litter
60 collection (Ryu et al., 2010; Liu et al., 2015a) are recognised as the most accurate method. However,
61 leaf harvest and allometric equations methods need time-consuming, labour-intensive and destructive
62 sampling process, while litter collection is more feasible for temperate deciduous forests. Obviously, the
63 direct method is less applicable for large-scale and long-term LAI monitoring (Bequet et al., 2012;
64 Biudes et al., 2014). Indirect methods include plant canopy analyser (Licor LAI-2000), hemispherical or
65 fisheye photography (Macfarlane et al., 2007) and remote sensing (Biudes et al., 2014). The indirect
66 methods retrieve LAI value from light transmittance through canopies or from canopy image analysis.
67 For large scale LAI estimates, remote sensing is the effective method but requires validation with the
68 ground-based LAI data. It is still a challenge for LAI estimates on the ground at small scales due to the
69 problems of sampling strategies associated with accepted level of accuracy, time and cost consideration
70 (Richardson et al., 2009). Hemispherical photography is a relatively simple and easily operated method
71 among many indirect methods to retrieve LAI value at small scales (Demarez et al., 2008). Correction
72 of the effects of woody materials, clumping and zenith angles or exposure is critical for improving the
73 accuracy of LAI estimation (Liu et al., 2015b). Analysis software development and portable and timely
74 characteristics allow hemispherical photography to measure spatial heterogeneity and seasonal
75 variations of LAI in forests.

76 Forest canopy structure is highly complicate so LAI values show great temporal and spatial variations



77 at scales ranging from stand to global scale. For example, LAI values in the 7.9 ha plot of an old humid
78 temperate forest tended to increase spatially as elevation increased and showed a temporal variation
79 with plant phenology (Naithani et al., 2013). The spatial patterns of LAI values at stand scale were
80 significantly influenced by spatial distribution of tree species, which was dependent on topography and
81 soil types (Naithani et al., 2013). Coefficient of variations (CV) in LAI decreased as the scale increased
82 and LAI values did not have any relationship with biome type and climate patterns, but were influenced
83 by land use and land cover, terrain features, and soil properties at stand scale (Aragão et al., 2005). The
84 CV of LAI of three species (i.e. beech, oak and pine) had different degree spatial variations in 1 ha plot
85 at stand level (Bequet et al., 2012). LAI values in sagebrush displayed strong spatial patterns with the
86 time after disturbance and increased with stand age and total plant cover (Ewers & Pendall, 2007). The
87 LAI values derived from MODIS data (Huang et al., 2008; Myneni et al., 2002) revealed strong spatial
88 variations at global scale and the variations were correlated with latitude (Tian et al., 2004). At global
89 scale, temperature is the limiting factor for LAI under cool conditions while water plays a predominant
90 role under other conditions, and this pattern differed among plant functional types (Iio et al., 2014). The
91 factors that govern the spatial variations in LAI values at stand level include forest types, stand structure
92 (Bequet et al., 2012), climate (Shao & Zeng, 2011), topography, soil moisture condition (Breshears &
93 Barnes, 1999), and human disturbance and management activities (Huang & Ji, 2010). Although effects
94 of topography, soil properties (Naithani et al., 2013; Aragón et al., 2005) and stand character (Bequet et
95 al., 2012; Yao et al., 2015) on LAI values have been investigated in detail, how forest types, tree species



96 diversity and stand structure affect spatial heterogeneity and seasonal variations of LAI has not been
97 fully understood.

98 Chinese subtropical forests contain a diversity of tree species with complex canopy structure and
99 mostly grow on heterogeneous topography and soil condition. As a result, LAI in subtropical forests
100 may exhibit greatly spatial and seasonal variations, which is worthy of further investigation. However,
101 LAI data of subtropical forests are relative deficiency in the global database (see Asner et al., 2003). In
102 this study, we selected three different forests (i.e. *Pinus massoniana* - *Lithocarpus glaber* coniferous
103 and evergreen broadleaved mixed forests, *Choerospondias axillaris* deciduous broadleaved forests, and
104 *L. glaber* - *Cyclobalanopsis glauca* evergreen broadleaved forests), LAI values were measured by using
105 hemispherical photography. Spatial heterogeneity of LAI was investigated through geostatistics analysis
106 method. The generalised additive models (GAMs) were used to examine how tree species diversity and
107 stand characters affect LAI variations in the three forests. Specifically, the objectives of this study were:
108 (1) to examine differences and seasonal variations in LAI among three forests in subtropical China; (2)
109 to analyse spatial heterogeneity of LAI values within a specific forest; and (3) to identify how forest
110 types, species diversity and stand characters control the spatial heterogeneity and seasonal variations of
111 LAI values in three forests.

112

113 **2 Materials and methods**

114 **2.1 Study site description**



115 The study was carried out at the Dashanchong Forest Farm (latitude 28°23'58" - 28°24' 58" N,
116 longitude 113°17'46" - 113°19'08" E), Changsha County, Hunan Province, China. The Farm
117 experiences a humid mid-subtropical monsoon climate. Mean annual air temperature was between
118 16.6 °C to 17.6 °C, with a mean monthly minimum temperature of -11 °C in January and maximum
119 temperature of 40 °C in July. Mean annual precipitation ranged from 1412 mm to 1559 mm, mostly
120 occurring between April and August. The topography is characterized by a typical low hilly landscape
121 with an altitude between 55 m to 260 m above sea level. Soil type is designated as well-drained clay
122 loam red soil developed on slate and shale rock, classified as Alliti-Udic Ferrosols, corresponding to
123 Acrisol in the World Reference Base for Soil Resource (IUSS Working Group WRB, 2006). Evergreen
124 broadleaved forest is the climax vegetation of the region. As a result of human disturbance and
125 management activities, the Farm possesses a range of secondary forests dominated by different tree
126 species, including *P. massoniana* - *L. glaber* coniferous and evergreen broadleaved mixed forests, *C.*
127 *axillaris* deciduous broadleaved forests, and *L. glaber* - *C. glauca* evergreen broadleaved forests (Xiang
128 et al., 2015).

129

130 **2.2 Stand characteristics determination**

131 We established a permanent plot for each of three forests (i.e. 90 m × 190 m plot for *P. massoniana* -
132 *L. glaber* mixed forests, 100 m × 100 m plot for *C. axillaris* deciduous forests, and 100 m × 100 m plot
133 for *L. glaber* - *C. glauca* evergreen broadleaved forests). Each plot was divided into 10 m × 10 m



134 subplots, where tree species, diameter at breast height (DBH, cm), tree height (H, m), height under the
135 lowest live branch (m) and crown width (m) were measured for the individual stem with DBH larger
136 than 1 cm. Stand characteristics for the trees with DBH larger than 4 cm of the three forests were
137 presented in Table S1.

138 To identify the factors that control spatial heterogeneity of LAI values in the forests, we selected
139 individual trees with H larger than average height of each stand (see Table S1) and calculated their stem
140 number, average DBH, H, total basal area at breast height (BA), crown width, crown coverage,
141 biodiversity index, the proportion of BA of three functional group (coniferous, deciduous and evergreen
142 broadleaved species) to total stand BA within a subplot. Biodiversity index (BDI) was determined by
143 Shannon-Wiener index as the formula:

$$144 \quad BDI = -\sum P_i \ln P_i \quad (1)$$

145 where P_i is important value of i th species and is calculated by dividing the sum of relative abundance
146 degree (A_r) and relative dominance degree (D_r) of i th species within a subplot by two.

147

148 **2.3 Sampling design for LAI measurement**

149 At the centre of each subplot of the three forests, hemispherical photographs were taken using a LAI
150 measuring instrument (SY-S01A) throughout four measurement seasons, i.e. in April (spring), July
151 (summer) and October (autumn) in 2014 and January (winter) in 2015. The operation was carried out
152 below canopy with the fisheye lens 1.0 m above the ground (Manninen et al., 2009). We took the



153 photographs in the morning, dusk or cloudy to minimize influence of direct sunshine (Rich, 1990;
 154 Bequet et al., 2012). The images were processed and effective LAI values (L_e) were recorded by the
 155 plant canopy analysis system of the LAI measuring instrument. To obtain accurate LAI (L), the
 156 correction was made to L_e based on previous theory (Chen, 1996):

$$157 \quad L = \frac{(1 - \alpha)L_e\gamma_E}{\Omega_E} \quad (2)$$

158 where α is the ratio of woody to total area and reflects the contribution of woody materials to L_e . Ω_E is
 159 the clumping index that quantifies the effect of foliage clumping beyond shoots level. γ_E is the needle to
 160 shoot area ratio and quantifies the effect of foliage clumping within shoots.

161 Photoshop Software (Adobe Photoshop CS5, Adobe Systems Incorporated, North America) was used
 162 to calculate α . After total pixel number of L_e image was determined, the Clone Stamp Tool in the
 163 software was used to replace the woody materials with surrounding of non-woody materials and to
 164 obtain the pixel number and recorded as LAI of leaves (LAI_{leaf}). The value of α was calculated
 165 accordingly:

$$166 \quad \alpha = (L_e - LAI_{leaf})/L_e \quad (3)$$

167 The logarithm averaging method proposed by Lang and Xiang (1986) was applied to calculate Ω_E :

$$168 \quad \Omega(\theta) = \frac{\ln[P(\bar{\theta})]}{\ln[P(\theta)]} = \frac{n \ln[P(\bar{\theta})]}{\sum_{k=1}^n \ln(P_k(\theta))} \quad (4)$$

169 where $P(\theta)$ is the average gap fraction (expressed without the bar in the text), $\ln[P(\theta)]$ is the logarithm
 170 average of the gap fraction, $P_k(\theta)$ is the gap fraction of segment k . For deciduous and evergreen



171 broadleaved species, $\gamma_E=1.0$, but for coniferous species, γ_E is always greater than 1.0, but we ignored the
172 effect of needle to shoot area on LAI in this study.

173

174 2.4 Data analysis

175 The minimum, maximum, mean value, standard deviation and coefficient of variation (CV) were
176 calculated for the LAI data in the three forests. Two-way analysis of variance (ANOVA) was used to
177 detect effects of forest types and measurement seasons on LAI values. The LAI data in the three forests
178 were tested for normal distribution using the K-S test ($p<0.05$). We used domain method to identify the
179 specific values and replaced them with normally maximal values and if the data did not meet normal
180 distribution, the transformation was applied till the statistical assumption was met. Most values required
181 natural logarithm transformation to meet assumptions of normality. The exception is for *L. glaber* - *C.*
182 *glauca* in April which was cosine transformed and *L. glaber* - *C. glauca* in November which was
183 artan-transformed.

184 To investigate spatial heterogeneity of LAI values at four seasons measured in the three forests,
185 semivariance function was calculated as the following formula:

$$186 \quad \gamma(h) = \frac{1}{2N(h)} \sum_{i=1}^{N(h)} [Z(x_i) - Z(x_i + h)]^2 \quad (5)$$

187 where $\gamma(h)$ is semivariance value of lag distance h , $N(h)$ is the number of pair data for lag distance h ,
188 $Z(x_i)$ and $Z(x_i + h)$ represent LAI values at coordinate x_i and (x_i+h) (Rossi et al., 1992). Based on the
189 semivariogram plotting $\gamma(h)$ values against h variable, the appropriate models were fitted and we



190 obtained the values of nugget (C_0), sill (C_0+C), range (A_0) (Ewers & Pendall, 2007) and the ratio
191 [$C/(C_0+C)$] that reflected the degree of spatial autocorrelation of LAI values in a forest. Because spatial
192 autocorrelation and semivariogram theory make unbiased optimal estimation for regional variables in a
193 limited area (Bivand et al., 2013), Kriging interpolation method was used to predict unknown LAI
194 values in the forests from the data measured and to produce spatial distribution map of LAI values for
195 the three forests at four seasons.

196 Because the largest amount of defoliated leaves occurs in January and leaves fully expand in July in
197 subtropical forests, we chose LAI values measured in January and July in three forests as response
198 variable. Stepwise regression was used to select the factors that significantly affect LAI variations. The
199 factors include forest types, species diversity (species richness and biodiversity index) and stand
200 characters (stem number, average DBH, H, BA, crown width, crown coverage, the proportion of two
201 functional groups (deciduous and evergreen broadleaved species) to total stand BA). Stepwise
202 regression showed that BA, crown coverage, crown width, the proportion of deciduous species to total
203 stand BA and forest types significantly influenced LAI values measured in January, whereas species
204 richness, stem number, crown coverage and forest types significantly affected LAI values measured in
205 July (Tables S2). However, residuals of stepwise regression did not meet the requirements of normal
206 distribution and homogeneity (Fig. S1 and Fig. S2). The generalised additive models (GAMs) have the
207 advantages to analyse complex and nonlinear relationships (Guisan et al., 2002; Austin, 2002; Wood,
208 2006). Therefore, we used GAMs to examine how the factors selected by stepwise regression affect LAI



209 values. The function of GAMs is the addition of many smooth functions and each smooth function has
210 an explanatory variable. The variance inflation factor (VIF), the ratio of the variance of regression
211 coefficient for a variable when fitting with all variables to the variance of regression coefficient for the
212 variable if fit on its own, was used to test the multi-collinearity of explanatory variables (James et al.,
213 2013). When the VIF of an explanatory variable is between 0 and 10, the variable was retained to the
214 model; otherwise, we discarded the variable (Shen et al., 2015). The Akaike information criterion (AIC)
215 or generalised cross validation (GCV) was used to determine whether the model was good or bad (Clark,
216 2013). The factors selected after multi-collinearity test were used for multi-factor analysis. After all the
217 possible models in multi-factor analysis, we determined the optimal model based on the significant
218 influence of all explanatory variables in the model with the smallest AIC or GCV (Dong et al., 2012).
219 Geostatistics analysis was performed with GS+ software (Gamma Design Software). Statistical analysis
220 and GAMs analysis were operated in R programme. The car packages were used to test
221 multi-collinearity and the gam packages were used to select the optimal model.

222

223 **3 Results**

224 **3.1 Variations of LAI values in three forests**

225 The LAI values varied with forest types and measurement seasons (Table 1). Generally, LAI differed
226 significantly for measurement seasons ($p < 0.001$), but LAI difference was not significant among forest
227 types ($p > 0.05$). Interactive effects of measurement seasons and forest types on LAI were significant



228 ($p < 0.01$). Among three forests, LAI in the *P. massoniana* - *L. glaber* forest had relatively low variations,
229 while LAI in the *L. glaber* - *C. glauca* forest had the highest variations. In the *P. massoniana* - *L. glaber*
230 forest, LAI showed the largest variations (the highest CVs) in October and the lowest variations (the
231 smallest CVs) in January. In the *C. axillaris* forest, the largest variation in LAI was found in April and
232 the lowest was found in January. In the *L. glaber* - *C. glauca* forest, LAI showed the largest variations
233 in April and had the lowest variations in July.

234 Mean LAI values in the three forests showed different seasonal variation patterns (Fig. 1). The *C.*
235 *axillaris* forest exhibited a unimodal pattern of seasonal variations, with the maximum mean LAI value
236 (3.11 ± 1.18) occurring in July and the minimum mean LAI value (1.28 ± 0.44) in January. In the *P.*
237 *massoniana* - *L. glaber* forest and *L. glaber* - *C. glauca* forest, the maximum mean LAI value both
238 occurred in October and the minimum mean LAI value appeared in January. During the growing season
239 (April and July), the *C. axillaris* forest had the highest mean LAI value and the *L. glaber* - *C. glauca*
240 forest had the lowest mean LAI value. During the non-growing season (October and January), the *L.*
241 *glaber* - *C. glauca* forest had the highest mean LAI value in January, while the *P. massoniana* - *L.*
242 *glaber* forest had the highest mean LAI value in October, the *C. axillaris* forest had the lowest mean
243 LAI values.

244 Mean α values in the three forests showed different seasonal variation patterns (Table 2). The *C.*
245 *axillaris* forest exhibited a unimodal pattern of seasonal variations in mean α value, with the maximum
246 mean α value occurring in January and the minimum mean α value in July. No obvious seasonal



247 variations were found for the mean α value in the *P. massoniana* - *L. glaber* forest and in the *L. glaber* -
248 *C. glauca* forest. Mean Ω_E values in the three forests were between 0.84-0.92, but they did not show
249 clear seasonal variations, and the standard deviations were small.

250

251 **3.2 Spatial heterogeneity of LAI values in three forests**

252 The semivariograms results for LAI in three forests during different measurement seasons were
253 summarised in Table 3. The spatially dependent variance [C] accounted for 88.9% - 98.4% of the total
254 variance [$C+C_0$] for LAI values measured in January in the three forests and also in April, July and
255 October in the *L. glaber* - *C. glauca* forest. This indicated the strong spatial autocorrelations of LAI
256 values at short distance. These LAI data were best fitted with gaussian model or exponential model ($r^2 >$
257 0.50).

258 Spatial autocorrelation range of LAI values differed among forests and measurement seasons (Table
259 3). In January, the largest spatial autocorrelation range was found in the *P. massoniana* - *L. glaber* forest,
260 and the lowest was found in the *C. axillaris* forest. In April, the largest spatial autocorrelation range of
261 LAI was found in the *C. axillaris* forest, and the lowest was found in the *P. massoniana* - *L. glaber*
262 forest. In July, the *P. massoniana* - *L. glaber* forest had the largest spatial autocorrelation range of LAI,
263 while the *C. axillaris* forest had the smallest spatial autocorrelation range. In October, the *L. glaber* - *C.*
264 *glauca* forest had the largest spatial autocorrelation range of LAI, while the *P. massoniana* - *L. glaber*
265 forest had the smallest spatial autocorrelation range. Seasonal changes of range showed one peak



266 pattern for *C. axillaris* forest and *L. glaber* - *C. glauca* forest, where the large range appeared in the
267 growing season (April and July) and the small range appeared in the non-growing season (October and
268 January).

269 Spatial distribution pattern of LAI values also varied with forest types and measurement seasons (Fig.
270 2). For example, LAI values in January in three forests exhibited obvious patch and heterogeneous
271 spatial distribution. In April and July, less spatial heterogeneity was found for LAI values in three
272 forests especially in the *P. massoniana* - *L. glaber* forest. In October, heterogeneous and patch spatial
273 distributions of LAI values appeared in the *L. glaber* - *C. glauca* forest, and banded spatial distributions
274 of LAI values obviously appeared in the *C. axillaris* forest.

275

276 3.3 Factors affecting LAI variations in three forests

277 The multi-collinearity test indicated that the factors with significant effects on LAI in January and
278 July selected by stepwise regression did not have multi-collinearity. Thus, BA, crown coverage, crown
279 width, the proportion of deciduous species to total stand BA and forest types were included as
280 explanatory variables in multi-factor analysis for LAI values measured in January in three forests (Table
281 4). The best fitted GAMs for LAI values in January was expressed as $LAI \sim s(BA, 2) + s(\text{crown}$
282 $\text{coverage}, 2) + s(\text{crown width}, 2) + s(\text{the proportion of deciduous species to total stand BA}, 2) + \text{factor}$
283 (forest types) . For LAI values measured in July, species richness, crown coverage, stem number and
284 forest types were included as explanatory variables in multi-factor analysis (Table 4). The best fitted



285 GAMs for LAI values in July was expressed as $LAI \sim s(\text{species richness}, 2) + s(\text{crown coverage}, 2) +$
286 $s(\text{stem number}, 2) + \text{factor}(\text{forest types})$.

287 The explanatory variables included in GAMs reflected their effects on or relationship with LAI
288 variations. Given that other variables were fixed, LAI measured in January tended to increase as BA
289 increased and showed a negative nonlinear relationship with crown coverage and a positive nonlinear
290 relationship with crown width. The LAI values tended to decrease as the proportion of deciduous
291 species to total stand BA increased (Fig. 3). Given that other variables were fixed, LAI measured in July
292 tended to increase as species richness increased and showed a positive nonlinear relationship with
293 crown coverage and a negative nonlinear relationship with stem number (Fig. 4).

294

295 **4 Discussion**

296 **4.1 Seasonal variations in LAI values among three forests**

297 LAI data in subtropical forests in southern China are less than that in other global regions (Asner et
298 al., 2003). This study provided seasonal LAI data in three subtropical forests that consist of contrasting
299 functional types of species. Mean LAI values in the three forests investigated in this study varied from
300 1.28 ± 0.44 to 3.28 ± 1.26 (Table 1). This result is close to LAI range (from 1.0 in winter to 4.0 in summer)
301 retrieved by remote sensing techniques from subtropical area of China during the period 2000 to 2010
302 (Liu et al., 2012). Compared with the LAI values estimated from allometric equations (Xiang et al.,
303 2016) and specific leaf area (SLA) at $40 \text{ m} \times 40 \text{ m}$ quadrat plots of this study (5.29-9.19), the LAI



304 values measured by hemispherical photography are low but significantly correlated ($r^2=0.40$ and
305 $p=0.035$). Previous studies (see Lopes et al., 2015) have proved the underestimation of LAI using
306 hemispherical photography. However, the hemispherical photography method is feasible to obtain LAI
307 data in forests and to investigate spatial and seasonal variations in LAI in forests (Coops et al., 2004;
308 Dovey & Toit, 2006).

309 The ratio of woody to total area (α) and the clumping index (Ω_E) have been recognised as the error
310 sources in LAI measurement by optical methods (Liu et al., 2015a; Br da, 2003; Chen et al., 1997). So
311 far these two parameters have been measured in Northeastern China (Liu et al., 2015a; Liu et al., 2015b)
312 but they are not suitable for LAI correction in subtropical forests. Also the literature about them in
313 subtropical forests has been rarely reported. Our results showed that mean α values in the three forests
314 varied from 0.04 ± 0.03 to 0.15 ± 0.09 (Table 2). The variations of α value are probably due to the seasonal
315 variations and spatial heterogeneity of canopy structure in the three forests. In general, the α values are
316 consistent with the amount of leaf litter. Our results showed that the large mean α values occurred in
317 autumn for the *P. massoniana* - *L. glaber* forest and the *C. axillaris* forest, but in spring and autumn for
318 the *L. glaber* - *C. glauca* forest (Table 2). This seasonal change of mean α values in three forests was
319 generally consistent with the amount of leaf litter collected by litter tap installed in the three forests
320 (Guo et al., 2015). The average Ω_E value (0.87) in this study is smaller than the values of mixed
321 broadleaved - korean pine forest in Northeastern China (Liu et al. 2015b) and this could be attributed to
322 the different region and forests. The values of α and Ω_E obtained in this study fill the gap of calibration



323 for optical measurement of LAI in subtropical forests.

324 Mean LAI values differed among the three forests and the differences were significant between the *C.*
325 *axillaris* forest and other two forests at a given measurement season. The *C. axillaris* forest had the
326 relatively high mean LAI value during the growing season but changed to the lowest mean LAI value
327 during the non-growing season. The change in mean LAI values in the *C. axillaris* forest was consistent
328 with the study of a deciduous species dominated forest reported by Naithani et al. (2013). It has been
329 reported that the forests consisting of different plant functional types of species showed different LAI
330 values (Asner et al., 2003; Iio et al., 2014). The differences and seasonal variations of LAI values in the
331 three forests could be attributed to floristic composition and phenological defoliation pattern of tree
332 species especially the deciduous species. The *C. axillaris* forest consisted of 74.15% deciduous species,
333 25.80% evergreen broadleaved species and 0.05% evergreen coniferous species while the proportions of
334 deciduous species were 10.05% and 25.70% respectively in the *P. massoniana* - *L. glaber* forest and the
335 *L. glaber* - *C. glauca* forest. Seasonal growth and defoliation of different functional types of species
336 lead to the change in leaf lifespan and foliage area (Niinemets et al., 2010) during different seasons
337 related to temperature and water availability, which are responsible for the unimodal pattern of seasonal
338 variations in mean LAI values. This agrees with the results from Liu et al. (2012) that the highest LAI
339 was found in summer (July), followed by autumn (October) and spring (April), and the lowest was
340 found in winter (January).

341



342 **4.2 Spatial heterogeneity and its controlling factors of LAI values within a forest**

343 Semivariograms of LAI values in the three forests were fitted with spherical models, gaussian models,
344 exponential models or linear models (Table 3). Based on the fitted models, the degree of spatial
345 autocorrelation could be evaluated. Spatial autocorrelation is weak when the determination coefficient
346 (r^2) of the best-fitted semivariogram model is less than 0.5 (Duffera et al., 2007). The ratio $[C/(C_0+C)]$
347 is also used to describe the degree of spatial autocorrelation. The ratio between 0 and 0.25 indicates a
348 weak spatial autocorrelation, between 0.26 to 0.75 means moderate and larger than 0.75 means strong
349 (Lopez-Granados et al., 2004). Spatial autocorrelation of LAI in this study varied with forests and
350 measurement seasons (Table 3). Strong spatial autocorrelation at short range for LAI values measured in
351 January in three forests indicated the sampling distance is reasonable for LAI variables within the
352 spatial range (Liu et al., 2008). On the contrary, weak autocorrelation within spatial autocorrelation
353 range indicated that more samples and smaller sampling intervals should be taken to determine spatial
354 dependency of LAI, such as LAI measured in April in the *P. massoniana* - *L. glaber* forest.

355 Spatial heterogeneity of LAI values was different in three forests and measurement seasons. Our
356 study respectively described spatial variations of LAI values by CV and analysis of geostatistics and the
357 results were basically consistent with each other. In general, the CVs of LAI values in three forests (in
358 particular *C. axillaris* forest) were higher for the period of leaf onset (April) and senescence (October)
359 than that for the period of leaf maturity (July) (Table 1). This reflects changes of leaves due to plant
360 phenology and is consistent with the study by Naithani (2013) that LAI became increasingly



361 homogenous from leaf onset to maturity, but became more heterogeneous from maturity to senescence.
362 As a result, heterogeneity degree of LAI values in three forests tended to dwindle from leaf
363 non-growing season to growing season (Fig. 2).

364 The complex hydrothermal environment results in complex vertical and horizontal variations of
365 canopy layer and formed the unique spatial heterogeneity of LAI values. The results of stepwise
366 regression and GAMs showed that forest types, species diversity and stand characters affected the
367 spatial heterogeneity of LAI values significantly in three forests. This finding that floristic composition
368 and stand characters affected LAI values measured in July is consistent with the previous study that LAI
369 values increased with species richness (Yao et al., 2015). The positive relationship between LAI values
370 in July and crown coverage is also in agreement with the findings reported by Bequet (2012) that large
371 trees (high DBH, tree height, crown length and crown cover) had high LAI values measured in July. The
372 negative relationship between LAI values in July and stem number probably could be explained by the
373 strong competition among tree species in the three forests with diverse species composition.

374 Up to now, the relationship of LAI variations measured in non-growing season with forest types and
375 stand characters has seldom reported. In this study, forest types, BA, crown width, crown coverage and
376 the proportion of deciduous species to total stand BA were the factors significantly affecting LAI
377 variations in January. Because large trees (high crown width and BA) had high LAI values and January
378 is the leaf senescence period of deciduous species, LAI values in January increased with BA and crown
379 width but decreased with deciduous species ratio. The fact that LAI values in January decreased with



380 increasing crown coverage could be explained that large crown coverage means more defoliation (in
381 particular deciduous species) in the forest in January.

382 Although the factors selected by regression could explain a small proportion (6%) of spatial
383 heterogeneity of LAI measured in July, the factors selected in January could explain 35% of the LAI
384 spatial heterogeneity (Table 4). The LAI heterogeneity also could be affected by that several other
385 factors, such as the topography (Naithani et al., 2012), soil features (Chloer et al., 2010), soil
386 temperature (Vitasse et al., 2009; Hardwick et al., 2015), microclimate, human activities and other
387 physicochemical properties. And yet, full leaf expansion of all tree species which covers up the effect of
388 other physicochemical properties on LAI leads to small difference in LAI in July. The effects of
389 environmental factors (such as temperate, rainfall, etc.) on LAI in the forests at fine scale should be
390 taken into account in the future studies.

391 Spatial heterogeneity of LAI in three forests can yield some useful information for sampling strategy
392 to accurate estimation of LAI by using indirect measurement. An optimal sampling strategy should
393 consider appropriate sampling plot size and the lowest sampling number as far as possible to obtain a
394 high sampling accuracy and a low sampling error (Bequet et al., 2012). Our study found that strong
395 spatial autocorrelations range were about 30m (Table 3), indicating that 30m range might serve as a
396 reference for sampling plot size to estimate LAI in subtropical forests. In addition, LAI heterogeneity
397 was closely related to floristic composition and stand characters, thus stand structural variables (BA or
398 DBH) are important for sampling strategy to measure LAI in forests (Bequet et al., 2012).



399

400 **5 Conclusions**

401 This study measured LAI in three subtropical forests using hemispherical photography method in
402 four seasons and offered reliable data to analyse spatial and seasonal variations of LAI in the three
403 forests. Our results indicated that LAI differed greatly with forests and measurement seasons. Seasonal
404 variations of LAI occurred in the three forests reflect defoliation phenomenon due to plant phenology.
405 LAI values in the three forests exhibited different spatial autocorrelation in four seasons. Obvious patch
406 distribution pattern of LAI values was found in the three forests during the non-growing seasons and
407 this pattern gradually dwindled in the growing seasons. While BA, crown coverage, crown width, the
408 proportion of deciduous species to total stand BA and forest types significantly affected the spatial
409 variations in LAI values in January, species richness, crown coverage, stem number and forest types
410 significantly affected the spatial variations in LAI values in July. These findings supplement LAI data
411 for global synthesis and provide useful information for sampling strategies to accurate LAI estimates
412 and simulating the models of forest production and hydrological cycle in subtropical forests.

413

414 **Acknowledgements**

415 This study was supported by the Specialized Research Fund for the Doctoral Program of Higher
416 Education (20124321110006), the National Natural Science Foundation of China (31570447 and
417 31300524), the Programme of State Forestry Special Fund for Public Welfare Sectors of China



418 (201304317), and the New Century Excellent Talents Program (NCET-06-0715). Thanks also go to
419 the staff of the administration office of Dashanchong Forest Farm, Changsha County, Hunan Province,
420 for their local support.

421

422 **References**

423 Alonzo, M., Bookhagen, B., McFadden, J. P., Sun, A., and Roberts, D. A.: Mapping urban forest leaf
424 area index with airborne lidar using penetration metrics and allometry, *Remote Sens. Environ.*, 162,
425 141-153, 2015.

426 Aragão, L. E., Shimabukuro, Y. E., Santo, F., and Williams, M.: Landscape pattern and spatial
427 variability of leaf area index in Eastern Amazonia, *For. Ecol. Manage.*, 211, 240-256, 2005.

428 Asner, G. P., Scurlock, J. M. O., and Hicke, J. A.: Global synthesis of leaf area index observations:
429 implications for ecological and remote sensing studies, *Global Ecol. Biogeogr.*, 12, 191-205, 2003.

430 Aston, A. R.: Rainfall interception by eight small trees, *J. Hydrol.*, 42, 383-396, 1979.

431 Austin, M. P.: Spatial prediction of species distribution: an interface between ecological theory and
432 statistical modelling, *Ecol. Model.*, 157, 101-118, 2002.

433 Bequet, R., Campioli, M., Kint, V., Muys, B., Bogaert, J., and Ceulemans, R.: Spatial variability of leaf
434 area index in homogeneous forests relates to local variation in tree characteristics, *For. Sci.*, 58,
435 633-640, 2012.

436 Biudes, M. S., Machado, N. G., Danelichen, V. H. M., Souza, M. C., Vourlitis, G. L., and Nogueira, J.



- 437 S.: Ground and remote sensing-based measurements of leaf area index in a transitional forest and
438 seasonal flooded forest in Brazil, *Int. J. Biometeorol.*, 58, 1181-1193, 2014.
- 439 Bivand, R. S., Pebesma, E. J., and Gómez-Rubio, V.: Applied spatial data analysis with R, Springer,
440 New York, USA, 2013.
- 441 Bréda, N. J. J.: Ground-based measurements of leaf area index: a review of methods, instruments and
442 current controversies, *J. Exp. Bot.*, 54, 2403-2417, 2003.
- 443 Breshears, D. D., and Barnes, F. J.: Interrelationships between plant functional types and soil moisture
444 heterogeneity for semiarid landscapes within the grassland/forest continuum: a unified conceptual
445 model, *Landscape Ecol.*, 14, 465-478, 1999.
- 446 Brooks, J. R., Meinzer, F. C., Warren, J. M., Domeo, J. C., and Coulombe, R.: Hydraulic redistribution
447 in a Douglas-fir forest: lessons from system manipulation, *Plant Cell Environ.*, 29, 138-150, 2006.
- 448 Brut, A., Rüdiger, C., Lafont, S., Roujean, J. L., Calvet, J. C., Jarlan, L., Gibelin, A. L., Albergel, C.,
449 Moigne, P. L., Soussana, J. F., Klumpp, K., Guyon, D., Wigneron, J. P., and Ceschia, E.:
450 Modelling LAI at a regional scale with ISBA-A-gs: comparison with satellite-derived LAI over
451 southwestern France, *Biogeosciences*, 6, 1389-1404, 2009.
- 452 Chen, J. M.: Optically-based methods for measuring seasonal variation of leaf area index in boreal
453 conifer stands, *Agric. For Meteorol.*, 80, 135-163, 1996.
- 454 Chen, J. M., Rich, P. M., Gower, S. T., Norman, J. M., and Plummer, S.: Leaf area index of boreal
455 forests: theory, techniques, and measurements, *J. Geophys. Res.*, 102, 29429-29443, 1997.



- 456 Chloer, P., Sea, W., Briggs, P., Raupach, M., and Leuning, R.: A simple ecohydrological model captures
457 essentials of seasonal leaf dynamics in semiarid tropical grasslands, *Biogeosciences*, 7, 907-920,
458 2010.
- 459 Clark, D. B., Olivas, P. C., Oberbauer, S. F., Clark, D. A., and Ryan, M. G.: First direct landscape-scale
460 measurement of tropical rain forest leaf area index: a key driver of global primary productivity,
461 *Ecology Letter*, 11, 163-172, 2008.
- 462 Clark, M.: Generalized additive models: getting started with additive models in R, Center of Social
463 Research, University of North Dame, Notre Dame, IN, USA, pp.13, 2013.
- 464 Crockford, R. H., and Richardson, D. P.: Partitioning of rainfall into throughfall, stemflow and
465 interception: effect of forest type, ground cover and climate, *Hydrol. Proc.*, 14, 2903-2920, 2000.
- 466 Coops, N. C., Smith, M. L., Jacobsen, K. L., Martin, M., and Ollinger, S.: Estimation of plant and leaf
467 area index using three techniques in a mature native eucalypt canopy, *Austral Ecology*, 29, 332-341,
468 2004.
- 469 Demarez, V., Duthoit, S., Baret, F., Weiss, M., and Dedieu, G.: Estimation of leaf area and clumping
470 indexes of crops with hemispherical photographs, *Agr. For. Meteorol.*, 148, 644-655, 2008.
- 471 Dong, X. H., Bennion, H. E., Maberly, S. C., Sayer, C. D., Simpson, G. L., and Battarbee, R. W.:
472 Nutrients exert a stronger control than climate on recent diatom communities in Esthwaite Water:
473 Evidence from monitoring and palaeolimnological records, *Freshwater Biol.*, 57, 2044-2056, 2012.
- 474 Dovey, S. B., and Toit, B. D.: Calibration of LAI-2000 canopy analyser with leaf area index in a young



- 475 eucalypt stand, *Trees*, 20, 273-277, 2006.
- 476 Duffera, M., White, J. G., and Weisz, R.: Spatial variability of Southeastern U. S. Coastal Plain soil
477 physical properties: implication for site-specific management, *Geoderma*, 137, 327-339, 2007.
- 478 Ewers, B. E., and Pendall, E.: Spatial patterns in leaf area and plant functional type cover across
479 chronosequences of sagebrush ecosystems, *Plant Ecol.*, 194, 67-83, 2007.
- 480 Facchi, A., Baroni, G., Boschetti, M., and Gandolfi, C.: Comparing optical and direct methods for leaf
481 area index determination in a maize crop, *J. Agri. Eng.*, 1, 27-34, 2010.
- 482 Global Climate Observing System (GCOS): Systematic Observation Requirements for Satellite-Based
483 Products for Climate Supplemental details to the satellite-based component of the Implementation
484 Plan for the Global Observing System for Climate in Support of the UNFCCC (2010 Update).
485 WMO/TD: 138. <http://www.wmo.int/pages/prog/gcos/Publications/gcos-154.pdf> (accessed on 13
486 November 2012), 2006..
- 487 Gonsamo, A., and Chen, J. M.: Continuous observation of leaf area index at Fluxnet - Canada sites,
488 *Agric. For. Meteorol.*, 189, 168-174, 2014.
- 489 Guisan, A., Edwards, Jr. T. C., and Hastie, T.: Generalized linear and generalized additive model in
490 studies of species distributions: Setting the scene, *Ecol. Model.*, 157, 89-100, 2002.
- 491 Guo, J., Yu, L. H., Fang, X., Xiang, W. H., Deng, X. W., and Lu, X.: Litter production and turnover in
492 four types of subtropical forests in China, *Acta Ecologica Sinica*, 35, 4668-4677, 2015. (in Chinese
493 with English abstract)



- 494 Hardwick, S. R., Toumi, R., Pfeifer, M., Turner, E. C., Nilus, R., and Ewers, R. M.: The relationship
495 between leaf area index and microclimate in tropical forest and oil palm plantation: Forest
496 disturbance drives changes in microclimate, *Agric. For. Meteorol.*, 201, 187-195, 2015.
- 497 Huang, D., Knyazikhin, Y., Wang, W., Deering, D. W., Stenberg, P., Shabanov, N., Tan, B., and
498 Myneni, R. B.: Stochastic transport theory for investigating the three-dimensional canopy structure
499 from space measurements, *Remote Sens. Environ.*, 112, 35-50, 2008.
- 500 Huang, M., and Ji, J. J.: The spatio-temporal distribution of LAI in China-the comparison with
501 mechanism model and remote sensing inversion, *Acta Ecol. Sinica*, 30, 3057-3064, 2010. (in
502 Chinese with English abstract)
- 503 Iio, A., Hikosaka, K., Anten, N. P. R., Nakagawa, Y., and Ito, A.: Global dependence of field-observed
504 leaf area index in woody species on climate: a systematic review, *Global Ecol. Biogeogr.*, 23,
505 274-285, 2014.
- 506 IUSS Working Group WRB: World Reference Base for Soil Resource 2006, In: *World Soil Resources*
507 *Reports No. 103*. 2nd ed. FAO, Rome, 2006.
- 508 James, G., Witten, D., Hastie, T., and Tibshirani, R.: *An introduction to statistical learning with*
509 *applications in R*. Springer, New York, 2013
- 510 Kross, A., McNairn, H., Lapen, D., Sunohara, M., and Champagne, C.: Assessment of RapidEYE
511 vegetation indices for estimation of leaf area index and biomass in corn and soybean crops, *Int. J.*
512 *Appl. Earth Obs. Geoinformation*, 34, 235-248, 2015.



- 513 Lang, A. R. G., and Xiang, Y.: Estimation of leaf area index from transmission of direct sunlight in
514 discontinuous canopies, *Agric. For. Meteorol.*, 35, 229-243, 1986.
- 515 Lee, K. S., Cohen, W. B., Kennedy, R. E., Maieringer, T. K., and Gower, S. T.: Hyperspectral versus
516 multispectral data for estimating leaf area index in four different biomes, *Remote Sens. Environ.*, 91,
517 508-520, 2004.
- 518 Liu, X. L., Zhao, K. L., Xu, J. M., Zhang, M. H., Si, B., and Wang, F.: Spatial variability of soil organic
519 matter and nutrients in paddy fields at various scales in southeast China, *Environ. Geol.*, 53,
520 1139-1147, 2008.
- 521 Liu, Y. B., Ju, W. M., Chen, J. M., Zhu G. L., Xing, B. L., Zhu, J. F., and He, M. Z.: Spatial and
522 temporal variations of forest LAI in China during 2000-2010, *Chin Sci Bull.*, 57, 2846-2856, 2012..
- 523 Liu, Z. L., Jin, G. Z., Chen, J. M., and Qi, Y. J.: Evaluating optical measurements of leaf area index
524 against litter collection in a mixed broadleaved-Korean pine forest in China, *Trees*, 29, 59-73,
525 2015a.
- 526 Liu, Z. L., Wang, C. K., Chen, J. M., Wang X. C., and Jin, G.Z.: Empirical models for tracing seasonal
527 changes in leaf area index in deciduous broadleaf forests by digital hemispherical photography, *For.*
528 *Eco. Manage.*, 351, 67-77, 2015b.
- 529 Lopes, D., Nunes, L., Walford, N., Aranha, J., Sette Jr, C., Viana, H., and Hernandez, C.: A simplified
530 methodology for the correction of Leaf Area Index (LAI) measurements obtained by ceptometer
531 with reference to *Pinus* Portuguese forests, *iForest–Biogeosci. Forest.*, 7: 186-192, 2015.



- 532 Lopez-Granados, F., Jurado-Exposito, M., Alamo, S., and Garcia-Torres, L.: Leaf nutrient spatial
533 variability and site-specific fertilization maps within olive (*Olea europaea* L.) orchards, *Eur. J.*
534 *Agron.*, 21, 209-222, 2004.
- 535 Macfarlane, C., Hoffman, M., Eamus, D., Kerp, N., Higginson, S., McMurtrie, R., and Adams, M.:
536 Estimation of leaf area index in eucalypt forest using digital photography, *Agr. For. Meteorol.*,
537 143, 176-188, 2007.
- 538 Manninen, T., Korhonen, L., Voipio, P., Lahtinen, P., and Stenberg, P.: Leaf area index (LAI) estimation
539 of boreal forest using wide optics airborne winter photos, *Remote Sens.*, 1, 1380-1394, 2009.
- 540 Mason, P. J., Manton, M., Harrison, D. E., Belward, A., Thomas, A. R., and Dawson, A.: The second
541 report on the adequacy of the global observing systems for climate in support of the UNFCCC.
542 GCOS-82, WMO/TD No. 1143; United Nations Environment Programme; International Council for
543 Science, World Meteorological Organization: Geneva, Switzerland, 2003, p. 74, 2003.
- 544 Myneni, R. B., Hoffman, S., Knyazikhin, Y., Privette, J. L., Glassy, J., Tian, Y., Wang, Y., Song, X.,
545 Zhang, Y., Smith, G. R., Lotsch, A., Friedl, M., Morisette, J. T., Votava, P., Nemani, R. R., and
546 Running, S. W.: Global products of vegetation leaf area and fraction absorbed PAR from year one
547 of MODIS data, *Remote Sens. Environ.*, 83, 214-231, 2002.
- 548 Naithani, K. J., Baldwin, D. C., Gaines, K. P., Lin, H., and Eissenstat, D. M.: Spatial distribution of tree
549 species governs the spatio-temporal interaction of leaf area index and soil moisture across a forested
550 landscape, *PLoS One*, 8(3), e58704, 2013.



- 551 Naithani, K. J., Ewers, B. E., and Pendall, E.: Sap flux-scaled transpiration and stomatal conductance
552 response to soil and atmospheric drought in a semi-arid sagebrush ecosystem, *J. Hydrol.*, 25,
553 176-185, 2012.
- 554 Niinemets, Ü.: A review of light interception in plant stands from leaf to canopy in different plant
555 functional types and in species with varying shade tolerance, *Ecol. Res.*, 25, 693-714, 2010.
- 556 Rich, P. M.: Characterizing plant canopies with hemispherical photographs, *Remote Sens. Rev.*, 5,
557 13-29, 1990.
- 558 Richardson, J., Moskal, L. M., and Kim H.: Modeling approaches to estimate effective leaf area index
559 from aerial discrete-return LIDAR, *Agr. For Meteorol.*, 149, 1152-1160, 2009.
- 560 Rossi, R. E., Mulla, D. J., Journel, Á. G., and Franz, E. H.: Geostatistical tools for modeling and
561 interpreting ecological spatial dependence, *Ecol. Monogr.*, 62, 277-314, 1992.
- 562 Ryu, Y., Nilson, T., Kobayashi, H., Sonnentag, O., Law, B. E., and Baldocchi, D. D.: On the correct
563 estimation of effective leaf area index: dose it reveal information on clumping effects, *Agric. For*
564 *Meteorol.*, 150, 463-472, 2010.
- 565 Shao, P., and Zeng, X. D.: Spatiotemporal relationship of leaf area index simulated by CLM3.0-DGVM
566 and climatic factors, *Acta Ecol. Sinica*, 16, 4725-4731, 2011. (in Chinese with English abstract)
- 567 Shen, C. C., Lei, X. D., Liu, H. Y., Wang, L., and Liang, W. J.: Potential impacts of regional climate
568 change on site productivity of *Larix olgensis* plantations in northeast China, *iForest-Biogeosci.*
569 *Forest.*, e1-10, 2015.



- 570 Smith, H.: Light quality as an ecological factor. In: Grace, J., E.D. Ford, and P.G. Jarvis (eds). Plants
571 under their atmospheric environment, Blackwell, Oxford, 93-110, 1981.
- 572 Sprintsin, M., Karnieli, A., Berliner, P., Rotenberg, E., Yakir, D., and Cohen, S.: The effect of spatial
573 resolution on the accuracy of leaf area index estimation for a forest planted in the desert transition
574 zone, *Remote Sens. Environ.*, 109, 416-428, 2007.
- 575 Tian, Y., Dickinson, R. E., Zhou, L., Zeng, X., Dai, Y., Myneni, R. B., Knyazikhin, Y., Zhang, X., Friedl,
576 M., Yu, H., Wu, W., and Shaikh, M.: Comparison of seasonal and spatial variations of leaf area
577 index and fraction of absorbed photosynthetically active radiation from moderate resolution imaging
578 spectroradiometer (MODIS) and common land model, *J. Geophys. Res.*, 109, D01103, 2004.
- 579 Vitasse, Y., Delzon, S., Dufréne, E., Pontailler, J. Y., Louvet, J. M., Kremer, A., and Michalet, R.: Leaf
580 phenology sensitivity to temperature in European trees: do within-species populations exhibit
581 similar responses, *Agric. For. Meteorol.*, 149, 735-744, 2009.
- 582 Wood, S.: *Generalized Additive Models: An introduction with R*, Chapman & Hall, CRC, Boca Raton,
583 FL, USA, 8-15, 2006.
- 584 Woodgate, W., Jones, S. D., Suarez, L., Hill, M. J., Armston, J. D., Wilkes, P., Soto-Berelov, M.,
585 Haywood, A., and Mellor, A.: Understanding the variability in ground-based methods for retrieving
586 canopy openness, gap fraction, and leaf area index in diverse forest systems, *Agric. For. Meteorol.*,
587 205, 83-95, 2015.
- 588 Xiang, W., Fan, G., Lei, P., Zeng, Y., Tong, J., Fang, X., Deng, X., and Peng, C.: Fine root interactions



589 in subtropical mixed forests in China depend on tree species composition, *Plant Soil*, 395, 335-349,
590 2015.

591 Xiang, W. H., Hou, Y. N., Ouyang, S., Zhang, S. L., Lei, P. F., and Li, J. X.: Development of allometric
592 equations for estimating tree component biomass of seven subtropical species in southern China,
593 *European Journal of Forest Research*, in review, 2016.

594 Yao, D. D., Lei, X. D., Yu, L., Lu, J., Fu, L. Y., and Yu, R. G.: Spatial heterogeneity of leaf area index of
595 mixed spruce-fir-deciduous stands in northeast China, *Acta Ecol. Sinica*, 1, 71-79, 2015. (in Chinese
596 with English abstract)

597

598

599

600

601

602

603

604

605

606

607

608



609 **Table 1** Descriptive statistical characteristics of LAI values measured during period from April 2014 to
 610 January 2015 in *P. massoniana* - *L. glaber*, *C. axillaris* and *L. glaber* - *C. glauca* forests (n=100).

611

Month	Forest type	Minimum value	Maximum value	Variance coefficient (%)	<i>P</i> value of K-S test	Data transformation
January	<i>P. massoniana</i> - <i>L. glaber</i>	1.29	4.03	27.5	0.021	0.275
	<i>C. axillaris</i>	0.53	2.38	34.0	0.260	
	<i>L. glaber</i> - <i>C.</i> <i>glauca</i>	0.43	6.98	40.2	0.018	0.243
April	<i>P. massoniana</i> - <i>L. glaber</i>	1.57	7.83	36.4	0.076	
	<i>C. axillaris</i>	1.34	8.33	47.0	0.047	0.535
	<i>L. glaber</i> - <i>C.</i> <i>glauca</i>	1.34	10.22	59.6	0.000	0.158
July	<i>P. massoniana</i> - <i>L. glaber</i>	1.56	8.16	38.0	0.003	0.075
	<i>C. axillaris</i>	1.73	8.17	37.8	0.166	
	<i>L. glaber</i> - <i>C.</i> <i>glauca</i>	1.68	7.58	33.1	0.010	0.170
October	<i>P. massoniana</i> - <i>L. glaber</i>	1.55	6.79	38.3	0.321	
	<i>C. axillaris</i>	0.37	6.51	44.1	0.102	
	<i>L. glaber</i> - <i>C.</i> <i>glauca</i>	1.49	7.88	49.3	0.000	0.212

612

613

614



615 **Table 2** Average woody to total leaf ration (α) and clumping index (Ω_E) values in *P. massoniana* - *L.*
 616 *glaber*, *C. axillaris* and *L. glaber* - *C. glauca* forests. Values in parenthesis are the standard deviation of
 617 α and Ω_E values (n=100).

618

Forest type	Month	α	Ω_E
<i>P. massoniana</i> - <i>L. glaber</i>	January	0.06 (0.04)	0.88 (0.09)
	April	0.08 (0.05)	0.87 (0.09)
	July	0.07 (0.04)	0.87 (0.09)
	October	0.09 (0.10)	0.85 (0.08)
<i>C. axillaris</i>	January	0.15 (0.09)	0.92 (0.08)
	April	0.07 (0.06)	0.85 (0.10)
	July	0.04 (0.03)	0.90 (0.07)
	October	0.14 (0.14)	0.87 (0.10)
<i>L. glaber</i> - <i>C. glauca</i>	January	0.07 (0.09)	0.87 (0.09)
	April	0.15 (0.07)	0.86 (0.09)
	July	0.05 (0.03)	0.87 (0.08)
	October	0.09 (0.08)	0.84 (0.09)

619

620

621

622

623

624

625

626



627 **Table 3** Semivariogram theoretical models and fitted parameters for LAI values in *P. massoniana* - *L.*
 628 *glaber*, *C. axillaris* and *L. glaber* - *C. glauca* forests.

629

Month	Forest type	Model	Nugget (C_0)	Sill (C_0+C)	$C/(C_0+C)$	Range (A_0/m)	r^2	RSS
January	<i>P. massoniana</i> - <i>L. glaber</i>	Exponential	0.0068	0.0614	0.889	27.00	0.607	9.762×10^{-5}
	<i>C. axillaris</i>	Exponential	0.0030	0.1820	0.984	13.80	0.504	1.219×10^{-4}
	<i>L. glaber</i> - <i>C.</i> <i>glauca</i>	Gaussian	0.0029	0.1178	0.975	15.42	0.888	3.468×10^{-5}
April	<i>P. massoniana</i> - <i>L. glaber</i>	Exponential	0.1220	0.7670	0.841	17.70	0.229	0.017
	<i>C. axillaris</i>	Linear	0.1760	0.1760	0.000	52.96	0.189	1.762×10^{-4}
	<i>L. glaber</i> - <i>C.</i> <i>glauca</i>	Exponential	0.0008	0.0152	0.951	26.40	0.978	2.290×10^{-7}
July	<i>P. massoniana</i> - <i>L. glaber</i>	Linear	0.0843	0.0843	0.000	92.69	0.074	1.383×10^{-4}
	<i>C. axillaris</i>	Exponential	0.1460	0.9340	0.844	17.70	0.258	0.017
	<i>L. glaber</i> - <i>C.</i> <i>glauca</i>	Exponential	0.0065	0.0684	0.905	22.80	0.951	5.781×10^{-6}
October	<i>P. massoniana</i> - <i>L. glaber</i>	Exponential	0.1620	1.6310	0.901	11.70	0.173	0.017
	<i>C. axillaris</i>	Spherical	0.0050	0.5830	0.991	11.90	0.000	1.870×10^{-3}
	<i>L. glaber</i> - <i>C.</i> <i>glauca</i>	Exponential	0.0005	0.0125	0.960	21.90	0.894	4.444×10^{-7}

630

631

632

633

634

635



636 **Table 4** Estimated coefficients of the generalised additive models (GAMs) for the factors with effects
 637 on LAI values measured in *P. massoniana* - *L. glaber*, *C. axillaris* and *L. glaber* - *C. glauca* forests.

638

Month	Parameter	F-value	p-value	r ²	AIC
January	s (BA,2)	15.146	1.236×10 ⁻⁴ ***	0.3496	654.30
	s (Crown width,2)	1.588	0.209		
	s (Crown coverage,2)	0.556	0.456		
	s (PDSB,2)	49.324	1.556×10 ⁻¹¹ ***		
	factor(Forest types)	44.355	< 2.2×10 ⁻¹⁶ ***		
July	s (Species richness,2)	3.165	0.076.	0.0551	677.85
	s (Stem number,2)	8.381	4.086×10 ⁻³ **		
	s (Crown coverage,2)	0.006	0.939		
	factor(Forest types)	2.475	0.086.		

639

640 The significance of the regressions (*p*) are ., *, **, *** for *p*<0.1, 0.05, 0.01, and 0.001, respectively

641

642

643

644

645

646

647

648



649 **Figure captions**

650 **Fig. 1** Seasonal variations of mean LAI values (with standard deviation) in *P. massoniana* - *L. glaber*, *C.*
651 *axillaris* and *L. glaber* - *C. glauca* forests. The values carrying with different letters indicate significant
652 differences ($p < 0.05$) among measurement seasons in a given forest.

653

654 **Fig. 2** Spatial heterogeneity map of LAI values interpolated through ordinary Kriging method for *P.*
655 *massoniana* - *L. glaber*, *C. axillaris* and *L. glaber* - *C. glauca* forests.

656

657 **Fig. 3** Partial effects of total stand basal area (BA, cm²), average crown width (m), crown coverage (m²),
658 the proportion of deciduous species to total stand BA (PDSB), and forest types (calculated for overstory
659 trees with height larger than average stand height) on the LAI values observed in January in *P.*
660 *massoniana* - *L. glaber*, *C. axillaris* and *L. glaber* - *C. glauca* forests.

661

662 **Fig. 4** Partial effects of species richness, individual stem number, crown coverage (m²) and forest types
663 (calculated for overstory trees with height larger than average stand height) on the LAI values observed
664 in July in *P. massoniana* - *L. glaber*, *C. axillaris* and *L. glaber* - *C. glauca* forests.

665

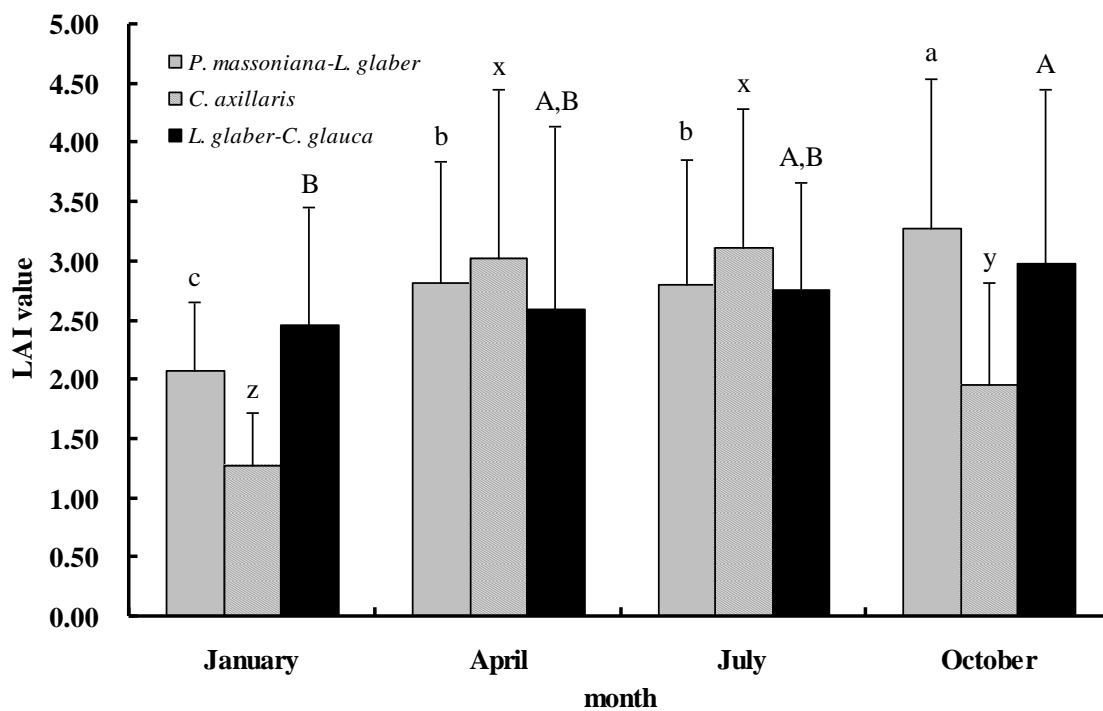
666

667



668 **Figure 1**

669



670

671

672

673

674

675

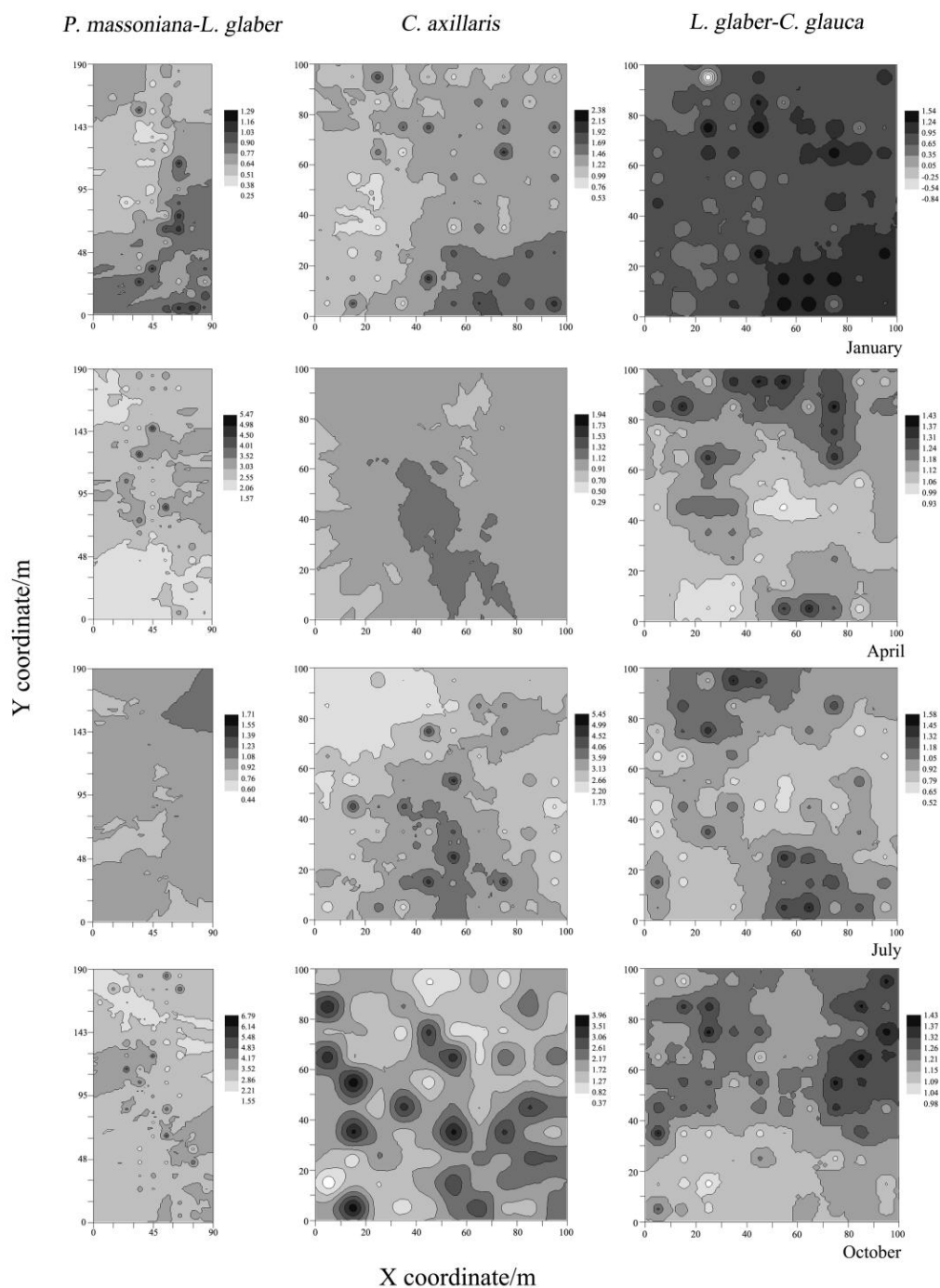
676

677

678



679 **Figure 2**

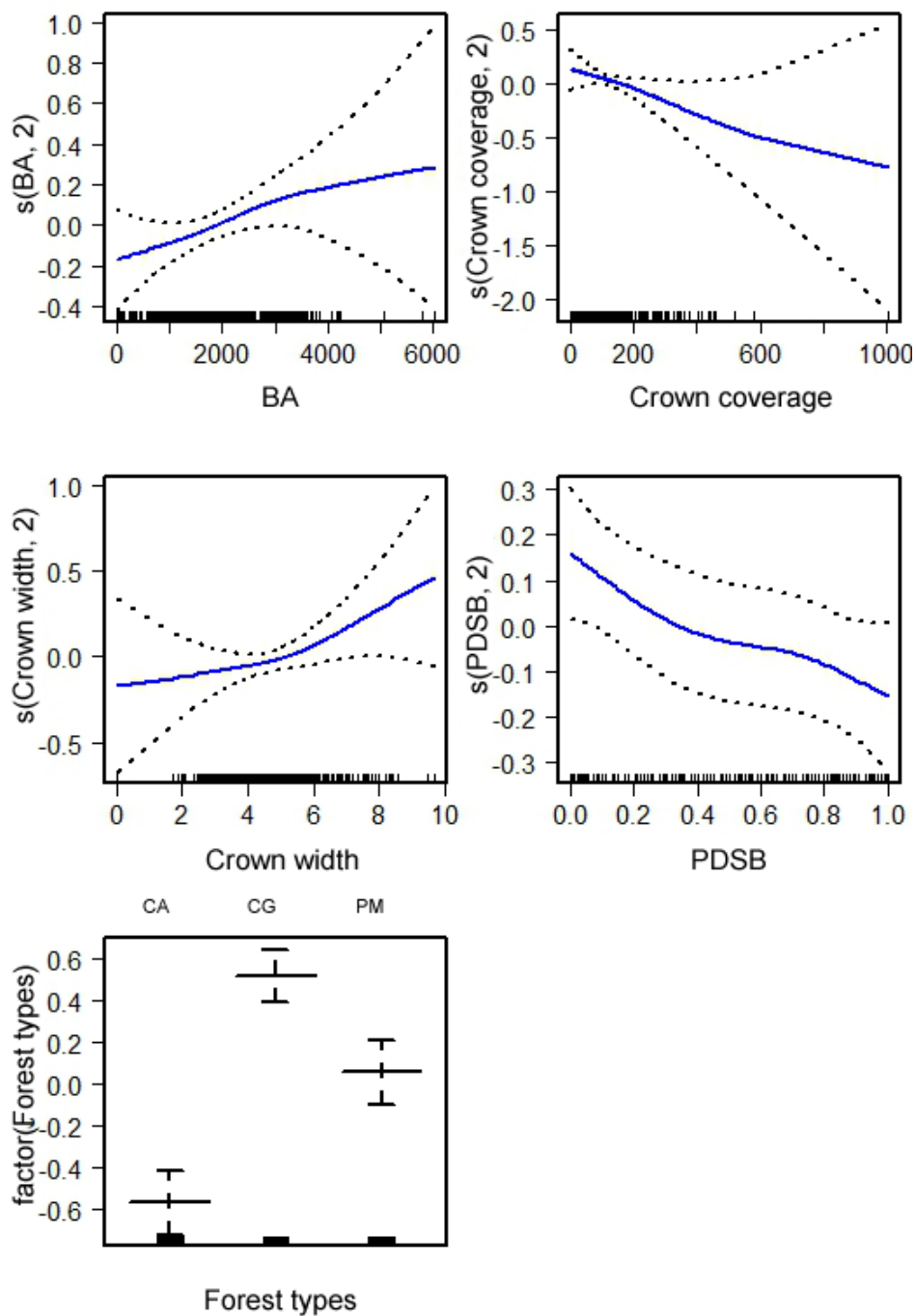


680

681



682 **Figure 3**

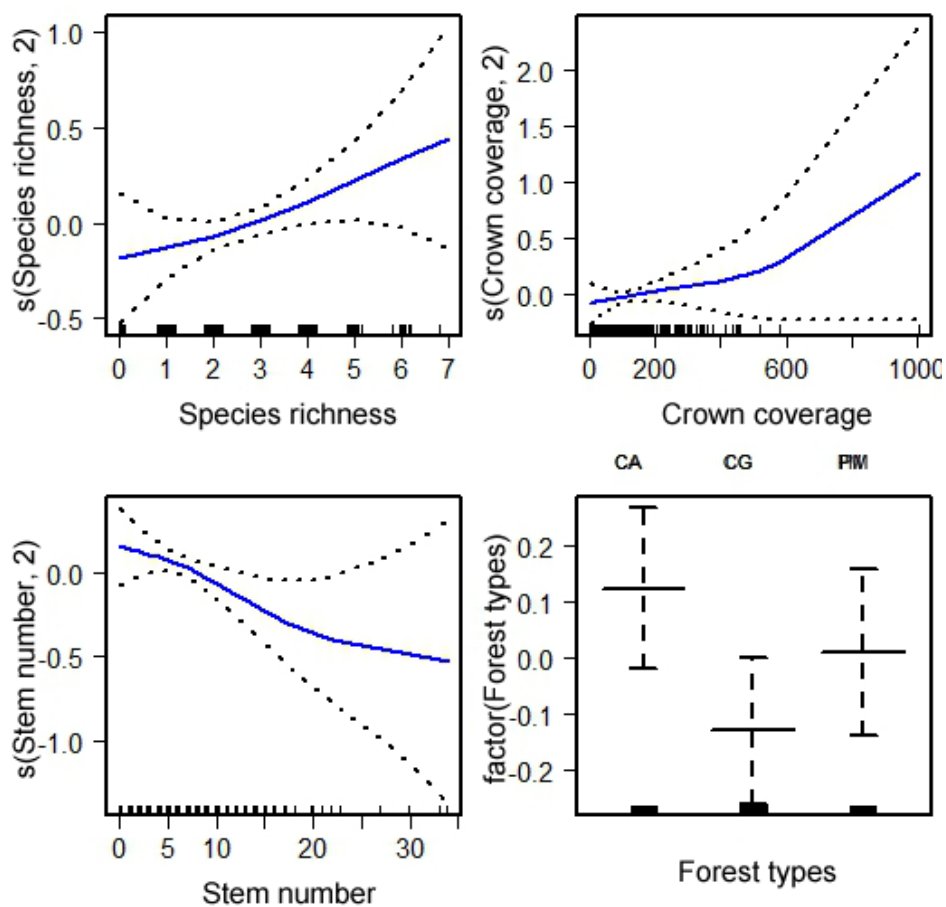


683

684



685 **Figure 4**



686

687

688

689